WARSAW UNIVERSITY OF TECHNOLOGY Index 351733
FACULTY OF CIVIL ENGINEERING
COMMITTEE FOR CIVIL AND WATER ENGINEERING
POLISH ACADEMY OF SCIENCES ISSN 1230-2945

DOI: 10.24425/ace.2026.157486

ARCHIVES OF CIVIL ENGINEERING

Vol. LXXII ISSUE 1 2026

pp. 465 –479

Research paper

Research on topology optimization considering anisotropy of additive manufactured structures

Jiaowei Feng[1], Hui Wang[2], Xukai Ren[3], Yan Li[4]

Abstract: The additive manufacturing process unique characteristics lead to the formation of structures with varying mechanical properties in different directions. However, current topology optimization methods often assume material isotropy, overlooking the anisotropy additive manufacturing materials. Hence, we propose a topology optimization method that accounts for additive manufacturing material anisotropy. We establish a local coordinate system to describe material anisotropy and integrate it into the SIMP variable density method, deriving the corresponding interpolation formula. The Kuhn–Tucker condition optimization criterion is applied to solve the problem, and an optimization program is developed. The method's feasibility and effectiveness are validated through numerical examples, and we extensively discuss the impact of material anisotropy and printing direction on topology optimization results. Research demonstrates that our proposed method is adept at solving both isotropic and anisotropic topology optimization problems. Moreover, the material degree of anisotropy and printing direction significantly influence topology optimization outcomes. Accounting for material anisotropy, the maximum principal stress difference in optimization results obtained under different printing directions can reach 52.26%.

Keywords: additive manufacturing, material anisotropy, SIMP variable density method, topology optimization

[1]MSc., Eng., Henan Technical Institute, School of Architecture and Engineering, No. 548. Zhengshang Road, 450042 Zhengzhou, China, e-mail: 591095285@qq.com, ORCID: 0009-0007-9334-3860

[2]PhD., Eng., Southeast University, School of Civil Engineering, No. 2. Southeast University Road, 211102 Nanjing, China, e-mail: WangHui0815@hotmail.com, ORCID: 0009-0006-1467-2440

[3]Assoc. Prof., MSc., Eng., Technical Institute, School of Architecture and Engineering, No. 548. Zhengshang Road, 450042 Zhengzhou, China, e-mail: 443027444@qq.com, ORCID: 0009-0008-9240-7575

[4]Eng., Zhengzhou Urban Development Group Co., Ltd., No. 2. Tongbo Road, 475007 Zhengzhou, China, e-mail: 289631086@qq.com, ORCID: 0009-0001-1461-1027

1. Introduction

Additive manufacturing (AM) technology, with its excellent molding capabilities, has significantly broadened the geometric shape range of manufacturable structures, thus attracting widespread attention and research from academia and industry [1, 2]. With the rapid development of AM technology, it provides a feasible way to manufacture topologically optimized configurations [3,4]. Topology optimization is an advanced structural optimization method that rationally and efficiently configures the material distribution in the design area based on preset load conditions, constraints, and performance requirements. However, the structures generated by topology optimization often have relatively complex geometric features, making it difficult to effectively implement traditional manufacturing processes such as casting and welding. AM technology has overcome the tool dependence and size limitations in traditional manufacturing, expanded the design space, and further promoted the development of topology optimization methods and their application in practical engineering [5–7]. The combined use of AM technology and topology optimization methods provides a new idea for the integration of structural design and manufacturing. Wang et al. [8] used topology optimization to obtain the optimal shape of the three-branch joints under vertical load, and manufactured the complex topology optimization joint by AM technology. Ye et al. [9] optimized and wire arc addictively manufactured the large-scale AM trusses of tubular cross-sections. The two complement each other and are very consistent with the development concept of the intelligent manufacturing era [10].

AM technology uses a layer-by-layer manufacturing method, which causes the molded material to exhibit obvious anisotropic characteristics [11]. The materials produced by Selective Laser Melting (SLM) technology have different strengths, Young's modulus and elongation at the break between the printing direction and the transverse direction (i.e., the plane perpendicular to the printing direction) [12]. For example, the print direction modulus of the nickel high-temperature alloy IN738LC prepared by SLM technology is 67% of the transverse modulus; the print direction modulus of the Ti6Al7Nb alloy is 138% of the transverse modulus [13, 14]. The anisotropy of materials formed by Wire and arc additive manufacturing (WAAM) technology is more obvious. Since the topology optimization configuration depends on the AM technology molding preparation, it is necessary to introduce the anisotropy of AM materials into the topology optimization so that the designed configuration has more practical application value. However, at this stage, the topology optimization method mainly uses isotropic and linear elastic materials. Recently, some experts have tried to study more complex material models, failure models, and structural or functional gradient materials constructed using multiple materials. Among them, a lot of research has been carried out on porous anisotropic materials, such as designing the unit cell structure of the lattice by topology optimization methods to control the volume of the lattice and optimize the micro-orientation [15–18]. This work studied and analyzed the anisotropy caused by the topologically optimized unit cell shape, but did not consider the anisotropy of the underlying material.

To explore the effect of the printing path on material anisotropy, some experts and scholars have studied the printing process, but have not introduced anisotropy into topology optimization [19]. Similarly, the optimal distribution of fiber orientation of extruded parts manufactured by extrusion molding, the optimal configuration of composite laminate structures

with angled layers, the optimal arrangement of material orientation distribution within the structure, and the optimal printing direction for a given design and load have all been studied, but the geometry of the structure has not been optimized at the same time [20, 21]. In topology optimization, the synergy between material anisotropy and printing direction has not been fully studied. Liu et al. [22] used the level set method to find that the printing direction affects the optimization results of structures with anisotropic elastic modulus, but only the shear modulus changes, while Young's modulus in the printing direction and transverse direction of the structure remains unchanged. Therefore, it is necessary to conduct further research on the influence of AM material anisotropy on the topology optimization results of structures.

This paper proposes a topology optimization method for AM material anisotropy. First, a local coordinate system describing the material anisotropy is constructed and introduced into the SIMP variable density method, and the corresponding interpolation formula is derived; then, the Kuhn–Tucker condition optimization criterion method is used to solve the problem, and the corresponding Matlab optimization program is compiled. Finally, the feasibility and effectiveness of the method are verified through three examples, and the influence of material anisotropy and printing direction on the topology optimization results is discussed in detail.

2. Anisotropy characterization of additive manufacturing materials

Material anisotropy refers to the fact that the physical, chemical, and mechanical properties of an object show different characteristics in different directions. Common indicators include elastic modulus, Poisson's ratio, yield strength, and ultimate strength. Due to the printing process and the manufacturing characteristics of layer-by-layer deposition, AM materials show anisotropy in elastic modulus, strength, and other indicators, especially the mechanical properties in the printing direction and perpendicular to the printing direction are different. In addition, related studies have shown that the mechanical properties of AM materials are usually the same within the deposition plane. For this reason, we refer to the characteristics of transversely isotropic materials and characterize the anisotropy of the elastic modulus of AM materials. This paper mainly studies the anisotropy of the elastic modulus of AM materials, which can better reflect the stiffness of the structure.

The anisotropy of the elastic modulus of AM materials is shown in Figure 1, which is manifested as different elastic moduli in the main direction 1 and the main direction 2 of the material. The direction of material 1 is the printing direction, represented by θ; the direction of material 2 is the transverse direction, which is perpendicular to the printing direction. The elasticity matrix $\mathbf{Q}$ in the physical coordinate system can be expressed as:

$$\mathbf{Q}(\theta) = \mathbf{R}(\theta)\hat{\mathbf{Q}}\mathbf{R}(\theta)^T \tag{2.1}$$

where $\hat{\mathbf{Q}}$ is the elasticity matrix in the material coordinate system. $\mathbf{R}$ represents the transformation matrix.

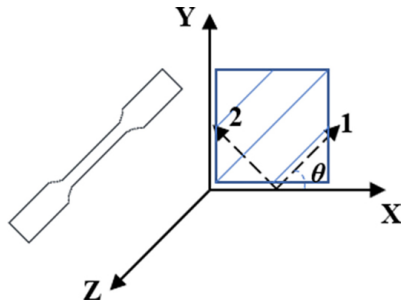

Fig. 1. Schematic diagram of the anisotropy of Young's modulus of AM materials

For anisotropic material model, a material off-angle θ is considered, and each vector in Eq. (2.1) is written as:

$$\hat{\mathbf{Q}} = \begin{bmatrix} \dfrac{E_1}{1-\nu_{12}\nu_{21}} & \dfrac{\mu_{12}E_2}{1-\nu_{12}\nu_{21}} & 0 \\ \dfrac{\nu_{12}E_2}{1-\nu_{12}\nu_{21}} & \dfrac{E_2}{1-\nu_{12}\nu_{21}} & 0 \\ 0 & 0 & G_{12} \end{bmatrix}, \quad \mathbf{R} = \begin{bmatrix} \cos^2\theta & \sin^2\theta & -2\cos\theta\sin\theta \\ \sin^2\theta & \cos^2\theta & 2\cos\theta\sin\theta \\ \cos\theta\sin\theta & -\cos\theta\sin\theta & \cos^2\theta-\sin^2\theta \end{bmatrix} \tag{2.2}$$

where E, ν and G denote the elastic modulus, Poisson's ratio and shear modulus, respectively, while the subscripts of the parameters denote the corresponding directions. And E and ν satisfy: $\dfrac{E_1}{\nu_{12}} = \dfrac{E_2}{\nu_{21}}$.

The degree of anisotropy of the elastic modulus of AM materials, α, is defined by Eq. (2.3):

$$\alpha = \frac{E_t - E_p}{E_p} \times 100\% \tag{2.3}$$

where E_t and E_p are the elastic moduli of the AM material in the lateral direction and printing direction, respectively; $\alpha = 0\%$ means that the material properties are isotropic; the larger the absolute value of α, the stronger the anisotropy of the elastic modulus of the AM material.

3. Topology optimization method for anisotropic additive manufacturing materials

3.1. Optimization model considering anisotropy of additive manufacturing materials

The topology optimization model considering the anisotropy of AM materials takes the material volume as a constraint and the maximum stiffness (minimum compliance) of the structure under static load as the optimization goal. Its mathematical model can be expressed as:

$$\begin{aligned} &\text{Find: } \rho \\ &\min: C = \mathbf{U}^T\mathbf{F} \\ &\text{s.t.} \begin{cases} \mathbf{K}(\rho, E_t, E_p)\mathbf{U}(\rho, E_t, E_p) = \mathbf{F} \\ \sum_{i=1}^{n} \rho_i v_i \le V^* = \varphi V_0 \\ 0 < \rho_{\min} \le \rho_i \le \rho_{\max} = 1 \end{cases} \end{aligned} \tag{3.1}$$

where ρ represents the topological density of the unit, that is, the design variable; C is the compliance of the structure; $\mathbf{U}$ represents the overall displacement matrix of the structure; $\mathbf{F}$ represents the overall load matrix of the structure; $\mathbf{K}$ represents the overall stiffness matrix of the structure; $\rho_{\min}$ represents the lower limit of the change of the unit topological density value; $\rho_{\max}$ represents the upper limit of the change of the unit topological density value; n represents the number of units; V_0 represents the total volume of the design domain; V^* represents the total volume of available material; φ represents the volume fraction.

3.2. The variable density method considering anisotropy of additive manufacturing materials

At present, the commonly used topology optimization methods for continuum structures include variable density method, level set method, bidirectional asymptotic structural optimization method, etc. [23]. This paper uses the SIMP variable density method, which has the advantages of simple program design, a small number of variables, and fast calculation speed, to optimize the structure. Its interpolation function is: Where a represents the elastic modulus of the i-th unit in the 1 and 2 directions; b represents the unit elastic modulus when the material in the i-th unit is completely retained; c represents the topological density of the i-th unit; represents the penalty factor, which is taken as d in this paper.

$$E_i = E_{i,0}(\rho_i)^p = \begin{cases} (E_t)_i = (E_t)_{i,0}\,(\rho_i)^p \\ (E_p)_i = (E_p)_{i,0}\,(\rho_i)^p \end{cases}, \quad (i = 1, 2, \ldots, n) \tag{3.2}$$

where E_i represents the elastic modulus of the i-th unit in the 1 and 2 directions; $E_{i,0}$ represents the unit elastic modulus when the material in the i-th unit is completely retained; ρ_i represents the topological density of the i-th unit; p represents the penalty factor, which is taken as $P = 3$ in this paper.

The Kuhn–Tucker (K–T) conditional optimization criterion method is then used to solve Eq. (3.1), yielding the following solution:

$$\frac{\partial C}{\partial \rho_i} + \lambda \frac{\partial \left(\sum_{i=1}^{n} \rho_i v_i - \varphi V_0 \right)}{\partial \rho_i} = 0 \tag{3.3}$$

where $\left(\dfrac{\partial C}{\partial \rho_i^{(h)}}\right)^*$ is the corrected compliance sensitivity; N_e is the unit set whose unit center is less than the filter radius from the i-th unit center, and the dot is the unit center point. H_{ej} is the weight of the j-th unit, and the calculation formula is:

$$H_{ej} = \max(0, r_{\min} - d(i,j)) \tag{3.4}$$

where $r_{\min}$ represents the filter radius, $r_{\min}$ is 1.5 times the unit size, and $d_{(i,j)}$ denotes the distance between the center points of units i and j.

3.3. Implementation of optimization methods

Algorithm 1

- Given design domain, boundary conditions, load conditions, uncertain variables, volume fraction.
- Generate FE mesh and assign initial vector of element relative density $\boldsymbol{\rho}$.
- Establish a material coordinate system.
- Set the convergence criteria of the SIMP method, i.e. the relative change of objective value is less than a given tolerance value ε_C $\left(\text{e.g. } \dfrac{C^{(n)} - C^{(n+1)}}{C^{(n)}} < \varepsilon_C = 0.01\right)$.
- Build the SIMP model. Begin and enter the loop.
- Finite element analysis, solving unit stiffness matrix, total structural stiffness, and displacement of each node.
- Calculate objective function, Lagrange multipliers, sensitivity analysis.
- Update vector of element relative density $\boldsymbol{\rho}$ using Kuhn–Tucker (K–T) optimization criteria.
- Convergence judgment: $\dfrac{C^{(n)} - C^{(n+1)}}{C^{(n)}} < \varepsilon_C = 0.01$. No, continue the loop. Yes, end the loop.
- Output the optimal solution.

4. Numerical examples

In this paper, Matlab is used to compile a topology optimization program that takes into account the anisotropy of AM materials. SLM technology is used as the manufacturing process of the example structure, and 316L stainless steel powder is used as the printing material. The mechanical properties of SLM-formed 316L stainless steel material given in reference [15] are used as the material parameters of the numerical example model for topology optimization research to verify the effectiveness and feasibility of the proposed method. AM material density $\rho = 7.85 \times 10^{-9}$ t/mm^3, elastic modulus $E_p = 210$ GPa, Poisson's ratio $\mu = 0.3$. The anisotropy degree α, E_t for a given material can be determined according to Eq. (2.3).

4.1. Cantilever Beam

Figure 2 shows the geometric characteristics and boundary conditions of the cantilever beam structure. It is divided into 3600 four-node elements. A fixed constraint is applied to the left end, and a load of $F = 50$ N is applied to the middle node of the right end. The natural coordinate system is indicated in the lower left corner. The anisotropy degree (α) of the cantilever beam material is set to 0%. Maximum stiffness is the optimization goal, with volume fraction as the constraint condition. The penalty factor (P) is set to 3.0, and checkerboard control is applied. Table 1 provides the specific topology optimization parameters for the cantilever beam.

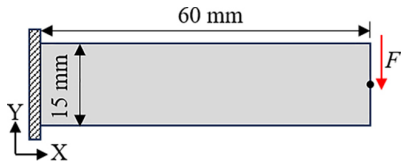

Fig. 2. Schematic diagram of the geometric information and boundary conditions of the cantilever beam

Table 1. Topology optimization parameters of cantilever beam.

Parameter	Value	Parameter	Value
Design variable	Unit density	Penalty factor	3.0
Optimization objectives	Maximizing stiffness	Filter radius	0.75 mm
Constraint condition	$\varphi = 0.3$	Anisotropy degree	0%
Density	7.85×10^{-9}	Poisson's ratio	0.3

The method proposed in this paper was used to carry out the topological optimization design of the cantilever beam, and the optimization iteration curve was obtained, as shown in Figure 3. It can be seen that during the 35 optimization iterations of the cantilever beam, the structure retained the material on its force transmission path and deleted the excess material, thereby achieving weight reduction.

In addition, the numerical theoretical solution of the Michell minimum truss shape is shown in Figure (4a) [24, 25]. Figure (4b) shows the result after 35 iterations of topology optimization. The two results exhibit certain similarities, verifying the feasibility and effectiveness of the proposed method. The differences arise because the Michell truss is solved using numerical theory, assuming an infinitely small unit grid, whereas the topology optimization method is constrained by a discretized grid, leading to variations in geometric shapes.

4.2. Tree Structure

To study the influence of anisotropy of AM materials on optimization results, a tree structure example is provided. The design area is a 10 ×7.5 m rectangle, with the upper part subjected to a vertical uniformly distributed load of $q = 2$ kN/m. The area with a thickness of

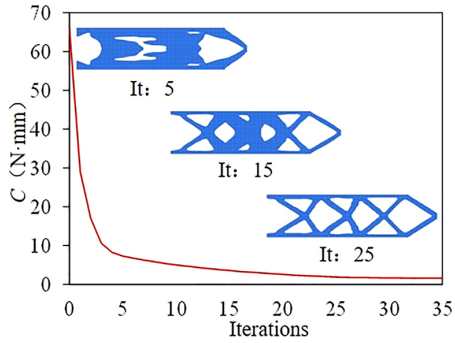

Fig. 3. Iteration Curve

(a) (b)

Fig. 4. Configuration comparison: (a) minimum truss scheme of Michell; (b) topology optimization results under the condition of $\alpha = 0\%$

0.3 meters in the upper part is considered as the roof structure and belongs to the non-optimized domain, as shown in Figure 5. The 0.4 m area in the middle of the bottom is the root fixing area of the tree structure.

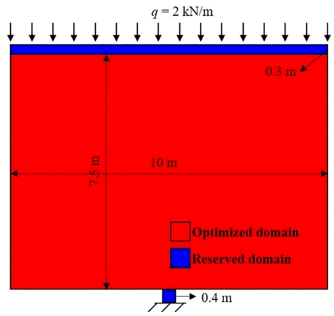

Fig. 5. Schematic diagram of geometric information and boundary conditions of the tree structure

When the material anisotropy degree α of the tree structure is –20%, the topology optimization design is performed with the printing directions θ = 0°, 30°, 45°, 60°, 90°, 120°, 135°, and 150°, and the results are shown in Figure 6. It can be seen that the geometric configuration of the optimization result obtained under the condition of material isotropy presents a symmetrical distribution, and the rods at the mid-span and both ends of the structure are thicker, which is consistent with its stress conditions, indicating that the result has a more reasonable structural distribution form. However, considering the anisotropy of the material, the symmetry of the geometric distribution of the structure will be lost as the AM printing

direction changes, and obvious thinner rods will appear in the results, affecting the performance and appearance of the optimization results.

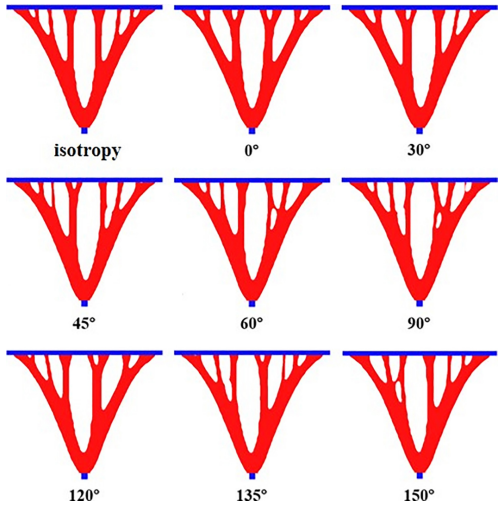

Fig. 6. Topology optimization structure under different printing directions ($\alpha = -20\%$)

4.3. L-beam

When $\alpha = 0\%$, that is, the material is isotropic, the effect of the printing direction on the topology optimization results is extremely low and can be ignored. However, the topology optimization of structures considering material anisotropy is a more complicated problem. Therefore, this example uses the L-beam as the research object to discuss in detail the influence of the printing direction and the degree of anisotropy on the topology optimization results. Figure 7 shows the geometric characteristics and boundary conditions of the L-beam structure. The structure is divided into 1200 four-node elements. A fixed constraint is applied to the top, and a load of $F = 500$ N is applied to the upper node on the right end. The natural coordinate system is indicated in the lower left corner. Minimum compliance is the optimization target. The volume fraction constraint is 0.3. The penalty factor P is set to 3.0, and checkerboard control is applied. The filter radius is set to 2.25 mm.

4.3.1. The influence of printing direction on topology optimization structure

When the material anisotropy degree α of the L-beam is 30%, the topology optimization design is performed with the printing directions $\theta = 0°$, 15°, 30°, 45°, 50°, 55°, 60°, 75°, and 90°, respectively. The results are shown in Figure 8. The material coordinate system is the green coordinate system in the figure (i.e., the printing direction). It can be seen that as the AM printing direction changes, the topological structure of the L-beam also changes accordingly. This is because the low modulus direction of the material deflects as the printing direction changes. The number, position, and size of the holes inside the topological structure vary with

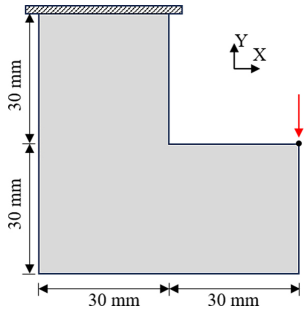

Fig. 7. Geometric characteristics and boundary conditions of L-beam structure

the printing direction. For example, when θ is 0°, 15°and 45°, there is only one hole inside the topological structure of the L-beam, and its position is similar but the size is different. When θ is 30°, there is no hole inside the topological structure. When θ is 50°, 55°, 60°, 75°, and 90°, there are 2 holes in the topological structure, but their sizes are different. In addition, when θ is 75°and 90°, the height of the topological configuration is lower than that of the other printing directions, and the material distribution is different. This shows that when the printing direction changes greatly, its influence on the topological optimization results is also more obvious; when the printing direction deflection angle is less than 15°, its influence on the topological optimization results is small.

To further verify the influence of AM printing direction on topology optimization, Table 2 presents the optimization results of L-beams at $\theta = 0°$, 45°, and 90° with an anisotropy degree $\alpha = -30\%$. The AM printing direction significantly influences the topology optimization results. Changes in the printing direction alter the distribution of structural materials, leading to variations in the mechanical properties of the structure. Table 2 shows that the maximum principal stress ($\sigma_{\max}$) of the optimization results can vary by up to 52.26% under different printing directions. Therefore, considering the printing direction in the AM process is essential.

Table 2. The influence of θ value on the optimization results of L-beam under the condition of $\alpha = 30\%$

Printing direction (θ)	**0°**	**45°**	**90°**
Stress cloud map	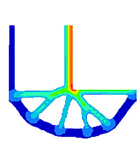	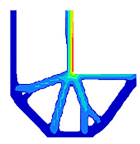	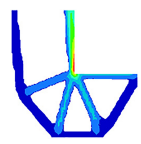
$\sigma_{\max}$	151.40 MPa	217.90 MPa	240.76 MPa
C	45.86 N·mm	46.19 N·mmm	43.79 N·mmm

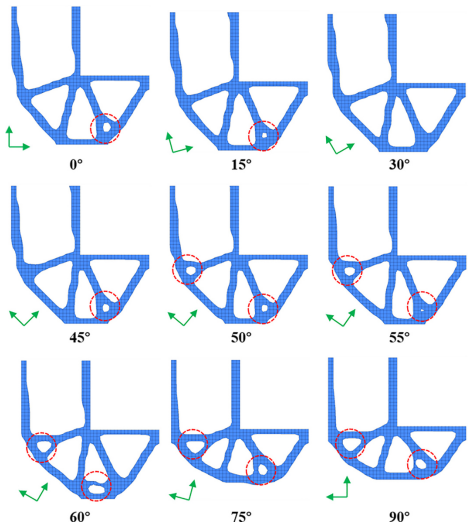

Fig. 8. Topology optimization structure under different printing directions (α = 30%)

4.3.2. The influence of material anisotropy on topology optimization structure

Figure 9 shows the topology optimization results for material anisotropy $\alpha = -40\%, -30\%, -20\%, -10\%, 0\%, 10\%, 20\%, 30\%$, and 40% when the printing direction angle of the L-beam is $\theta = 0°$. It can be seen that the topology optimization results considering the anisotropy of AM materials are different from those of isotropy (α = 0%). As the anisotropy increases, the difference in topological configuration becomes greater. When the degree of material anisotropy α < 0%, the elastic modulus in the transverse direction is smaller than in the printing direction. As E_t decreases (α increases), the vertical stiffness of the L-beam structure decreases. Therefore, to enhance vertical deformation resistance, the optimized material tends to distribute vertically. When α >0%, as E_t increases (α increases), the optimization result tends to distribute transversely.

Table 3 provides the compliance C, $\sigma_{\max}$, and maximum displacement $D_{\max}$ of the topological optimization results obtained under different α values under the condition of θ = 0%, which is convenient for quantitative analysis. It can be seen from Table 3 that with the increase of anisotropy, the compliance of the topological structure tends to decrease, that is, the structural stiffness is maximized. This is because the increase of E_t improves the structure's ability to resist deformation in the vertical direction, thereby increasing the overall stiffness of the structure. At the same time, the maximum global displacement of the topological structure also shows this trend. However, the change of the $\sigma_{\max}$ of the topology optimization result is opposite to that of C and $D_{\max}$. The reason is that when E_t is small, under the given optimization and boundary conditions, to ensure the overall stiffness of the structure, the material distribution of each rod is relatively uniform, and there is no large difference in the cross-sectional size of the rod. In particular, the cross-sectional area of the rod at the inner side ($\sigma_{\max}$) of the upper part of the L-beam structure has been greatly enhanced, thus avoiding stress concentration. It can be seen that the degree of anisotropy has a significant impact on the

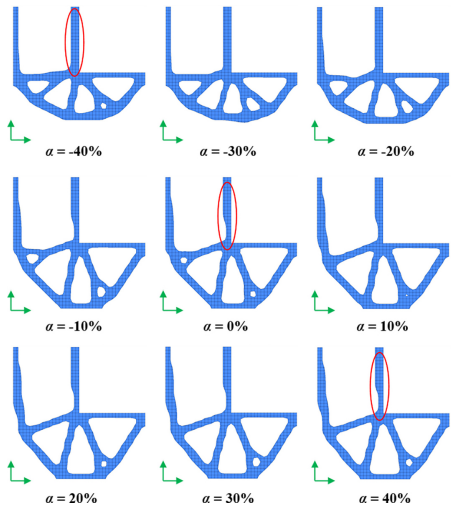

Fig. 9. Topology optimized structures with different degrees of anisotropy (θ = 0°)

mechanical properties of the topology optimization results. Whether E_t increases or decreases compared to E_p, it will change the material distribution of the topological structure and affect the mechanical properties of the structure.

Table 3. The influence of α value on the optimization results of L-beam under the condition of θ = 0°

Anisotropy degree (α)	***C* (N·mm)**	σ_{max} **(MPa)**	D_{max} **(mm)**
–40%	49.62	156.24	0.24
–30%	45.86	151.40	0.23
–20%	42.83	164.59	0.2
–10%	43.59	224.11	0.21
0	40.69	226.46	0.19
10%	38.13	233.22	0.17
20%	36.27	236.43	0.16
30%	34.6	237.75	0.15
40%	33.13	237.89	0.14

Figure 10, based on the data in Table 3, is presented to enhance intuitive understanding. In the figure, red indicates the performance indicators of the topology optimization results under isotropic conditions. The figure reveals significant differences in the mechanical properties of the topology optimization results under varying anisotropy conditions, highlighting the need to consider the anisotropy of AM materials. Additionally, Figure 10 shows that when the α is between –10% and 10%, the topology optimization results are less affected.

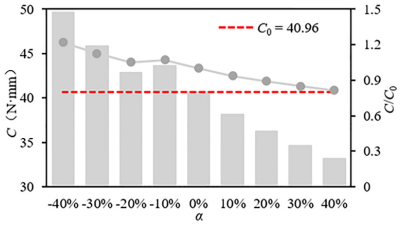

(a)

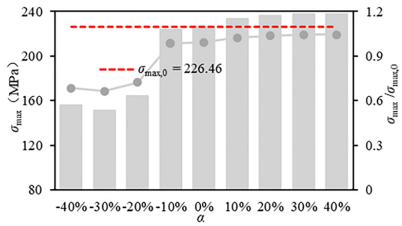

(b)

Continued on the next page

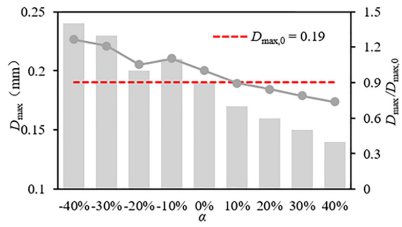

(c)

Fig. 10. Topology optimization results for different degrees of anisotropy ($\theta = 0°$): (a) C; (b) σ_{max}; (c) D_{max}

5. Conclusions

- This study proposes a topology optimization method that accounts for the anisotropic characteristics of AM materials. The results demonstrate that the proposed method effectively addresses topology optimization both under isotropic and anisotropic material conditions. The example further confirms the effectiveness of the proposed method.
- Changes in printing direction alter the material distribution, which subsequently affects the mechanical properties of the structure. The difference in σ_{max} of the optimization results can reach up to 52.26% under varying printing directions. When the $\theta < 15°$, its effect on topology optimization results is minimal.
- The material's degree of anisotropy significantly affects the optimization process. As anisotropy increases, the compliance of the topological structure decreases, and the maximum global displacement follows a similar trend. However, the σ_{max} shows the opposite trend to C and D_{max}. When the degree of anisotropy is between –10% and 10%, the optimization results are less affected.
- This paper presents a 2D numerical example using a single material. Future work will integrate deep learning to extend the proposed method to 3D structural examples involving multiple materials, such as AM metals and concrete, enhancing its generalizability.

Acknowledgements

This research was supported by the Youth Backbone Teacher Funding Project of Henan Technical Institute (Grant No. 2024-GGJS-T001), the Postgraduate Research£ŠPractice Innovation Program of Jiangsu Province (No. KYCX24_0427).

References

[1] T. Peng, Y. Zhu, M. Leu, and D. Bourell, "Additive manufacturing-enabled design, manufacturing, and lifecycle performance", *Additive Manufacturing*, vol. 36, art. no. 101646, 2020, doi: 10.1016/j.addma.2020.101646.

[2] E. Ulu, E. Korkmaz, K. Yay, B. Ozdoganlar, and L.B. Kara, "Enhancing the structural performance of additively manufactured objects", *Journal of Mechanical Design*, vol. 137, no. 11, art. no. 111410, 2015, doi: 10.1115/1.4030998.

[3] M. Bruggi, V. Laghi, and T. Trombetti, "Simultaneous design of the topology and the build orientation of Wire-and-Arc Additively Manufactured structural elements", *Computers & Structures*, vol. 242, art. no. 106370, 2021, doi: 10.1016/j.compstruc.2020.106370.

[4] J. Zou and X. Xia, "Topology optimization for additive manufacturing with strength constraints considering anisotropy", *Journal of Computational Design and Engineering*, vol. 10, no. 2, pp. 892–904, 2023, doi: 10.1093/jcde/qwad028.

[5] X. Song, Y. Pan, and Y. Chen, "Development of a low-cost parallel kinematic machine for multidirectional additive manufacturing", *Journal of Manufacturing Science and Engineering*, vol. 137, no. 2, art. no. 021005, 2015, doi: 10.1115/1.4028897.

[6] P. Singh and D. Dutta, "Offset slices for multidirection layered deposition", *Journal of Manufacturing Science and Engineering*, vol. 130, no. 1, art. no. 011011, 2008, doi: 10.1115/1.2783217.

[7] Y. Wang, Z. Luo, Z. Kang, and N. Zhang, "A multi-material level set-based topology and shape optimization method", *Computer Methods in Applied Mechanics and Engineering*, vol. 283, pp. 1570–1586, 2015, doi: 10.1016/j.cma.2014.11.002.

[8] L. Wang, W. Du, P. He, and M. Yang, "Topology optimization and This research was supported by the Youth Backbone Teacher Funding Project of Henan Technical Institute (Grant No. 2024-GGJS-T001), the Postgraduate Research£ŠPractice Innovation Program of Jiangsu Province (No. KYCX24_0427).3D printing of three-branch joints in treelike structures", *Journal of Structural Engineering*, vol. 146, no. 1, art. no. 04019167, 2020, doi: 10.1061/(ASCE)ST.1943-541X.0002454.

[9] J. Ye, P. Kyvelou, F. Gilardi, H. Lu, M. Gilbert, and L. Gardner, "An end-to-end framework for the additive manufacture of optimized tubular structures", *IEEE Access*, vol. 9, pp. 165476–165489, 2021, doi: 10.1109/ACCESS.2021.3132797.

[10] F. Chen, Y. Sun, S. Sun, D. Song, and Y. Liu, "Study on failure modes and calculation method of the cast steel joint with branches in treelike structure", *Archives of Civil Engineering*, vol. 70, no. 1, pp. 589–604, 2024, doi: 10.24425/ace.2024.148930.

[11] H. Wang, Z. He, and E. Zhou, "Collaborative optimization of structural topology and printing direction for anisotropy in additive manufacturing", *Journal of Mechanical Engineering*, vol. 59, no. 17, pp. 220–231, 2023.

[12] Y. Zhou and Y. Zhao, "Research progress and statistical analysis on the mechanical properties of selective laser melting additive manufacturing of stainless steel", *Journal of Building Structures*, vol. 42, no. 06, pp. 15–25, 2021.

[13] E. Chlebus, B. Kuźnicka, T. Kurzynowski, and B. Dybała, "Microstructure and mechanical behaviour of Ti-6Al-7Nb alloy produced by selective laser melting", *Materials Characterization*, vol. 62, no. 5, pp. 488–495, 2011, doi: 10.1016/j.matchar.2011.03.006.

[14] K. Kunze, T. Etter, J. Grässlin, and V. Shklover, "Texture, anisotropy in microstructure and mechanical properties of IN738LC alloy processed by selective laser melting (SLM)", *Materials Science and Engineering: A*, vol. 620, pp. 213–222, 2015, doi: 10.1016/j.msea.2014.10.003.

[15] Y. Zhao, R. Fan, Y. Liu, and Z. Wang, "Mechanical properties of 316L stainless steel prepared by wire arc additive manufacturing technology", *Journal of Building Structures*, vol. 44, no. 08, pp. 207–216, 2023.

[16] X. Huang, Y. Li, S. W. Zhou, and Y.M. Xie, "Topology optimization of compliant mechanisms with desired structural stiffness", *Engineering Structures*, vol. 79, pp. 13–21, 2014, doi: 10.1016/j.engstruct.2014.08.008.

[17] G. Zhang, L. Li, and K. Khandelwal, "Topology optimization of structures with anisotropic plastic materials using enhanced assumed strain elements", *Structural and Multidisciplinary Optimization*, vol. 55, no. 6, pp. 1965–1988, 2016, doi: 10.1007/s00158-016-1612-1.

[18] K. Ghabraie, "An improved soft-kill BESO algorithm for optimal distribution of single or multiple material phases", *Structural and Multidisciplinary Optimization*, vol. 52, no. 4, pp. 773–790, 2015, doi: 10.1007/s00158-015-1268-2.

[19] J. Liu and H. Yu, "Concurrent deposition path planning and structural topology optimization for additive manufacturing", *Rapid Prototyping Journal*, vol. 23, no. 5, pp. 930–942, 2017, doi: 10.1108/RPJ-05-2016-0087.

[20] C. Dapogny, R. Estevez, A. Faure, and G. Michailidis, "Shape and topology optimization considering anisotropic features induced by additive manufacturing processes", *Computer Methods in Applied Mechanics and Engineering*, vol. 344, pp. 626–665, 2019, doi: 10.1016/j.cma.2018.09.036.

[21] A.M. Mirzendehdel, B. Rankouhi, and K. Suresh, "Strength-based topology optimization for anisotropic parts", *Additive Manufacturing*, vol. 19, pp. 104–113, 2018, doi: 10.1016/j.addma.2017.11.007.

[22] J. Liu, "Guidelines for AM part consolidation", *Virtual and Physical Prototyping*, vol. 11, no. 2, pp. 133–141, 2016, doi: 10.1080/17452759.2016.1175154.

[23] T. Nomura, et al., "General topology optimization method with continuous and discrete orientation design using isoparametric projection", *International Journal for Numerical Methods in Engineering*, vol. 101, no. 8, pp. 571–605, 2015, doi: 10.1002/nme.4799.

[24] H. Wang, W. Du, Y. Zhao, Y. Wang, and M. Yang, "Optimization and experimental research of treelike joints based on generative design and powder bed fusion", *Engineering Structures*, vol. 278, art. no. 115564, 2023, doi: 10.1016/j.engstruct.2022.115564.

[25] H. Wang, W. Du, Y. Zhao, Y. Wang, R. Hao, and M. Yang, "Joints for treelike column structures based on generative design and additive manufacturing", *Journal of Constructional Steel Research*, vol. 184, art. no. 106794, 2021, doi: 10.1016/j.jcsr.2021.106794.

Received: 2024-08-29, Revised: 2024-11-18